Available online at www.sciencedirect.com
ScienceDirect
European Journal of Cell Biology 86 (2007) 473–487
European Journal of Cell Biology
www.elsevier.de/ejcb

Analysis of the axial filament in spicules of the demosponge *Geodia cydonium*: Different silicatein composition in microscleres (asters) and megascleres (oxeas and triaenes)

Werner E.G. Müller[a,*], Ute Schloßmacher[a], Carsten Eckert[a], Anatoli Krasko[a], Alexandra Boreiko[a], Hiroshi Ushijima[b], Stephan E. Wolf[c], Wolfgang Tremel[c], Isabel M. Müller[a], Heinz C. Schröder[a]

[a] *Institut für Physiologische Chemie, Abteilung Angewandte Molekularbiologie, Universität Mainz, Duesbergweg 6, D-55099 Mainz, Germany*
[b] *Department of Developmental Medical Sciences, Institute of International Health, Graduate School of Medicine, The University of Tokyo, 7-3-1 Hongo, Bunkyo-ku, Tokyo 113-0033, Japan*
[c] *Institut für Anorganische Chemie, Universität Mainz, Duesbergweg 10-14, D-55099 Mainz, Germany*

Received 18 April 2007; received in revised form 9 June 2007; accepted 12 June 2007

Abstract

The skeleton of the siliceous sponges (Porifera: Hexactinellida and Demospongiae) is supported by spicules composed of bio-silica. In the axial canals of megascleres, harboring the axial filaments, three isoforms of the enzyme silicatein (-α, -β and -γ) have been identified until now, using the demosponges *Tethya aurantium* and *Suberites domuncula*. Here we describe the composition of the proteinaceous components of the axial filament from small spicules, the microscleres, in the demosponge *Geodia cydonium* that possesses megascleres and microscleres. The morphology of the different spicule types is described. Also in *G. cydonium* the synthesis of the spicules starts intracellularly and they are subsequently extruded to the extracellular space. In contrast to the composition of the silicateins in the megascleres (isoforms: -α, -β and -γ), the axial filaments of the microscleres contain only one form of silicatein, termed silicatein-α/β, with a size of 25 kDa. Silicatein-α/β undergoes three phosphorylation steps. The gene encoding silicatein-α/β was identified and found to comprise the same characteristic sites, described previously for silicateins-α or -β. It is hypothesized, that the different composition of the axial filaments, with respect to silicateins, contributes to the morphology of the different types of spicules.

Keywords: Sponges; Porifera; *Geodia cydonium*; Silicatein; Collagen; Morphogenesis

Introduction

The sponges (phylum Porifera) are classified according to their anatomy/morphology and their skeleton into three classes; the phylogenetically oldest Hexactinellida and the Demospongiae, that both comprise a siliceous skeleton and the class of Calcarea, which

*Corresponding author. Tel.: +49 6131 392 5910; fax: +49 6131 392 5243.
E-mail address: wmueller@uni-mainz.de (W.E.G. Müller).
URL: http://www.biotecmarin.de/ (W.E.G. Müller).

0171-9335/$ - see front matter © 2007 Elsevier GmbH. All rights reserved.
doi:10.1016/j.ejcb.2007.06.002

possesses a skeleton built of calcium carbonate (Kruse et al., 1997, 1998). The sponge skeletal elements, the spicules, are traditionally separated into the categories of microscleres and megascleres (see Uriz et al., 2003) which are in the siliceous sponges synthesized from amorphous silicate (see Simpson, 1984). The two categories of the spicules are distinguished from each other not only by their size but also by their role in the skeletal organization (see Uriz et al., 2003). In demosponges, the megascleres form the skeletal framework and are embedded in a highly organized filamentous collagen network (Garrone, 1978; Eckert et al., 2006) while the microscleres are widely scattered within the sponge mesohyl (see Uriz et al., 2003). At higher magnification the sponge collagen appears as "striated fibrils" both in demosponges and hexactinellids (Imhoff and Garrone, 1983; Diehl-Seifert et al., 1985; Swatschek et al., 2002). The individual collagen fibrils have a diameter of approximately 23 nm (Diehl-Seifert et al., 1985) and form twisted bundles (Garrone et al., 1973; Junqua et al., 1974; Exposito et al., 2002; Ehrlich and Worch, 2007).

In the past few years the formation of the megascleres has been thoroughly studied in demosponges, e.g. *Suberites domuncula* (Müller et al., 2005a, 2006a; Schröder et al., 2006) and *Tethya aurantium* (Shimizu et al., 1998; Cha et al., 1999). Initially megascleres are formed intracellularly in special vesicles around an axial filament; after first siliceous layers are built the spicules are extruded into the extracellular space where the subsequent layers of silica allow the thickening growth (Müller et al., 2005a; Schröder et al., 2006, 2007) and also the elongation of the spicules (Müller et al., 2006c). An important finding was presented by the group of Morse (Shimizu et al., 1998; Cha et al., 1999) who showed that the spicules of the demosponges are mainly synthesized by an enzyme termed silicatein, which allows/facilitates the synthesis of silica from monomeric *ortho*-silicic acid. In marine demosponges two isoforms of silicatein genes have been identified, silicatein-α and -β in *T. aurantium* (Cha et al., 1999) and in *S. domuncula* (Krasko et al., 2000, 2002; Müller et al., 2006a), while in freshwater sponges more than five isoforms have been found (Müller et al., 2007a). The silicatein molecules exist in the axial canals of the spicules, where they form the axial filament. In addition, silicatein protein is present on the surface of the spicules where it mediates their lamellar thickening (Müller et al., 2006a). It is interesting to note that even in Calcarea the spicules, are formed discontinuously by appositional layering (Sethmann and Wörheide, 2007).

Collagen has been directly, or indirectly, implicated in silica biosynthesis. A direct interaction between collagen and "silicon/silicate" structures has been recently proposed; in addition it was suggested that collagen might be involved in "silicon" speciation/condensation (Eglin et al., 2006). Furthermore, using the glass sponge *Hyalonema sieboldi* experimental evidence has been presented that a fibrillar protein matrix in the silica shell of the spicules is crucial for the biomineralization process (Ehrlich et al., 2006; Ehrlich and Worch, 2007).

It has already been described by Lieberkühn (1856) for the sponge *Spongilla lacustris* and by Sollas (1888) for *Cydonium magellani* (family Geodina) that also microscleres are formed intracellularly. At later stages, most microscleres exist extracellularly, where they reach their final shapes and sizes. Subsequently, Schmidt (1862) and von Lendenfeld (1912) presented first reports demonstrating that the microscleres (asters) from *Caminus vulcani* are formed around a star-ray of filamentous protrusions which result in the globular sterrasters. The asters, during the stage when they exist extracellularly, are surrounded by a filigree network of collagen fibrils, as has been demonstrated by Simpson et al. (1985), suggesting that these fibrils might contribute to the morphogenesis of those spicules.

Until now no data are available about the composition of the axial filament in microscleres of siliceous sponges and hence also not on possible differences/distinctions between the silicatein(s) in microscleres and in megascleres. This question is of prime interest for the understanding of the development of sizes and shapes of the spicules, since they have species-specific forms. Spicules are only initially formed intracellularly, where their size and form can be controlled by the function of set(s) of proteins which are under direct influence of a differential gene expression. However, in the extracellular spaces such form-directing processes are only scarcely understood. Recently we proposed that the morphology of spicules, especially if the process proceeds extracellularly, is mediated by self-assembly, via fractal intermediates (Müller et al., 2007b). This view is based on a report which suggests that covalently linked monomers (dimers) of silicateins are the nuclei for the fractal intermediates during filament formation (Murr and Morse, 2005). We succeeded, after the elaboration of mild extraction conditions, to demonstrate that the silicatein molecules of the spicules can be re-assembled to characteristic filaments (Müller et al., 2007b).

To approach the question about a possible role of silicatein as a form-guiding molecule for the filigree spicules, we have selected the demosponge *Geodia cydonium* which comprises besides megascleres also microscleres since from this species a series of molecular genetic data has already been collected in the past, e.g. integrin (Pancer et al., 1997) or aggregation molecules (Blumbach et al., 1999), which helps to implement the data better into a genomic regulatory system. In addition, and most importantly, this sponge species is built of two types of spicules, the larger megascleres (the two types of oxeas, the protriaenes and the anatriaenes)

and the smaller microscleres (sterrasters and oxyasters (Arndt, 1935)). In the present study, we separated the microscleres from the megascleres and determined their molecular composition of the axial filaments. Surprisingly we found that – in contrast to the pattern in megascleres – the axial filament in the microscleres contains only one silicatein molecule. The cDNA for this protein was cloned and the deduced polypeptide was analyzed. From these results we deduce that a differential composition of the axial filaments with respect to the silicatein(s) contributes to the formation of the sizes and forms of spicules.

Materials and methods

Chemicals, materials and enzymes

Restriction enzymes, total RNA Isolation kit and reagents for the RACE procedure were purchased from Invitrogen (Carlsbad, CA, USA); TRIzol reagent from GibcoBRL (Grand Island, NY, USA); Hybond-N^+ nylon membrane from Amersham (Little Chalfont, Buckinghamshire, UK).

Sponges and spicules

Specimens of the marine sponge *Geodia cydonium* (Porifera, Demospongiae, Astrophorida) were collected in the Northern Adriatic near Rovinj (Croatia), and then kept in aquaria in Mainz (Germany). Frozen material was cut into 2–3 mm^3 cubes and soaked in nitric acid/sulfuric acid (1:4 v/v) for 2 days to obtain clean spicules. These were then rinsed in distilled water until the pH was 6 and then additionally treated in an ultrasound water bath. The separation of the spicules into micro- and megascleres was achieved first by differential sedimentation (the megascleres sedimented after about 3 min and the microscleres after 6 min); final separation was by filtration through a sieve (mesh size 68 μm). By this procedure almost pure microsclere and megasclere fractions were obtained. According to Uriz (2002) and Arndt (1935), *G. cydonium* contains as microscleres sterrasters and oxyasters and as megascleres oxeas and triaenes (protriaenes and anatriaenes).

Spicules and extract

After air-drying of the isolated, cleaned spicules, they were treated with 50 ml hydrofluoric acid (1 M HF/4 M NH_4F; pH 5) until the siliceous surfaces of the spicules were completely dissolved (Shimizu et al., 1998). This solution was dialyzed (3-times; at 4 °C for 4 h each) against 5 l 50 mM Tris–HCl (pH 8.8; 15% glycerol [v/v], 1 mM ethylenediaminetetraacetic acid, 150 mM NaCl). The thus isolated axial filaments were used both for sodium dodecyl sulfate polyacrylamide gel electrophoresis (SDS-PAGE) and Western blotting.

Light microscopic inspections were performed with an AHBT3 light microscope (Olympus).

SDS-PAGE and Western blot analysis

Protein samples were prepared from the axial filaments obtained after complete dissolution of the spicules with HF. Samples of 25 μg protein were dissolved in loading buffer (Roti-Load; Roth, Karlsruhe, Germany), boiled for 5 min and then subjected to 10% polyacrylamide gel electrophoresis, containing 0.1% SDS. After separation the gels were washed in 10% methanol (supplemented with 7% acetic acid) for 30 min and then stained in Coomassie brilliant blue as described (Müller et al., 2005b).

For Western blot analysis, the polypeptides were transferred to PVDF membranes (Millipore-Roth, Karlsruhe, Germany) and reacted with polyclonal anti-silicatein antibodies (PoAb [PoAb-aSilic, #N365]; from rabbits) that had been raised against the silicatein from *S. domuncula* as described earlier (Müller et al., 2005b). Where described the blots were incubated with polyclonal anti-collagen antibodies (PoAb-aCol, #N349; from rabbits) that had been raised against the complete recombinant collagen from *S. domuncula* (accession no. AJ252241 [collagen-1]; Schröder et al., 2000). The PVDF membranes were then rinsed in TBS-T (20 mM Tris–HCl [pH 7.6], 137 mM NaCl, 0.1% Tween-20) and incubated for 1 h with PoAb-aSilic (1:1000 dilution), or PoAb-aCol (1:600) diluted in TBS-T buffer, supplemented with 5% non-fat dry milk and 1.5% bovine serum albumin. Membranes were washed three times in TBS-T and then incubated for 1 h with anti-rabbit IgG (alkaline phosphatase conjugate; 1:2000 dilution; Sigma). The immunocomplexes were visualized with the chromogenic substrate system NBT/BCIP (Roth). In controls, pre-adsorbed PoAb-aSilic or PoAb-aCol (100 μl antibodies were pre-incubated with 20 μg recombinant silicatein rSILIC_SUBDO or recombinant collagen rCOL_SUBDO) was used. With these antibody preparations no signal could be seen in Western blots (Schröder et al., 2006). Protein size standard "Dual Color" (Roth) was used to estimate the size of the proteins.

Two-dimensional (2D) gel electrophoresis

The procedure for the 2D gel electrophoresis (IEF) was performed as described (Coligan et al., 1998; Müller et al., 2005b). In brief, IEF was carried out using a PROTEIN-IEF chamber (Bio-Rad, München, Germany) and immobilized pH gradient (IPG) strips (ReadyStrip IPG

Strip, pH 3–10, Bio-Rad). The protein samples containing 100 µg protein were mixed with rehydration buffer (8 M urea, 0.4% ampholytes, 60 mM DL-dithiothreitol, 0.002% bromophenol blue) and then loaded onto the strips (Coligan et al., 1998). The proteins were focused and subsequently size separated (10% SDS-PAGE). Staining of proteins was performed with Coomassie brilliant blue.

Electron microscopy

For scanning electron microscopic (SEM) analysis, samples were mounted onto stubs (carbon adhesive Leit-Tabs No. G 3347 [Plano, Wetzlar, Germany]). After sputtering with a 10 nm thin layer of gold in argon plasma (Bal Tec Med 020 coating system; Bal Tec, Balzers, Liechtenstein) the specimens were inspected with a Zeiss DSM 962 Digital Scanning microscope (Zeiss, Aalen, Germany).

For transmission electron microscopic analysis (TEM), sponge tissue samples were cut into pieces (1 mm^3), incubated in 0.1 M phosphate buffer (supplemented with 2.5% glutaraldehyde and 0.82% NaCl [pH 7.4]) and then washed in 0.1 M phosphate/1.75% NaCl buffer (pH 7.4) at room temperature. After treating the samples with 1.25% $NaHCO_3$, 2% OsO_4 and 1% NaCl, they were dehydrated with ethanol. The dried samples were incubated with propylene oxide, fixed in propylene oxide/araldite (2:1), covered with pure araldite and hardened at 60 °C for 2 days prior to cutting to 60 nm ultrathin slices (Ultracut S; Leica, Wetzlar, Germany). The samples were transferred onto coated-copper grids and analyzed with a Tecnai 12 microscope (FEI Electron Optics, Eindhoven, The Netherlands).

Identification of the *G. cydonium* silicatein cDNA

Reverse transcription polymerase chain reaction (PCR) was performed to obtain the cDNA from *G. cydonium* for silicatein (*GCSILCA*). Total RNA from tissue of a specimen was extracted with TRIzol reagent (Invitrogen) as described (Grebenjuk et al., 2002). This RNA was reverse-transcribed using oligo(dT) primers and SuperScript-II reverse transcriptase (Invitrogen). After first-strand synthesis, the resulting cDNA preparation was diluted to one-tenth with H_2O and an aliquot of 2 µl was subjected to PCR. The reaction was performed in a volume of 50 µl using primers designed against the conserved region of the silicatein genes, isolated from *S. domuncula*. The following primer set was used; the forward primer: 5′-CAGGGAGACTG-TGGTGCTAGCTATGC-3′ (directed against the amino acids stretch in silicatein-α [accession no. AJ272013] from *S. domuncula* N-QGDCGASYA-C; aa_{132}–aa_{140}), as well as the reverse primers: 5′-AGCAATTCCA-CACTGGTTGTACTTGTT-3′ (against aa_{314}–aa_{322} in silicatein-α from *S. domuncula*; N-NKYNQCGIA-C). PCR reaction conditions were: initial denaturation at 95 °C for 3 min, then 35 amplification cycles each at 94 °C for 30 s, a gradient from 57 to 60.5 °C (0.1 °C increase every cycle) 20 s, 70 °C for 90 s, followed by a final incubation for 10 min at 72 °C. Samples were then subjected to an automated DNA sequencer (LICOR 4200). The sequence obtained for the *G. cydonium* silicatein (*GCSILICA*) was 573 bp long. A fragment of the expected size was obtained, cloned into pCRII-TOPO vector (Invitrogen) and sequenced using standard procedures. Completion of the cDNA was achieved by the RACE technique. The clone encoding *G. cydonium GCSILICA* is 1088 long (excluding the poly(A) tail).

Sequence analyses

The sequence was analyzed with computer programs Blast (2005; http://www.ncbi.nlm.nih.gov/blast/blast.cgi) and FASTA (2005; http://www.ebi.ac.uk/fasta33/). Multiple alignments were performed with CLUSTAL W Ver. 1.6 (Thompson et al., 1994). Phylogenetic trees were constructed on the basis of amino acid (aa) sequence alignments by neighbor-joining, as implemented in the "Neighbor" program from the PHYLIP package (Felsenstein, 1993). The distance matrices were calculated using the Dayhoff PAM matrix model as described (Dayhoff et al., 1978). The degree of support for internal branches was further assessed by bootstrapping (Felsenstein, 1993). The graphic presentations were prepared with GeneDoc (Nicholas and Nicholas, 1997).

Northern blotting

RNA was extracted from liquid-nitrogen pulverized sponge tissue with TRIzol reagent. Total RNA (5 µg) was electrophoresed through 1% formaldehyde/agarose gels and blotted onto Hybond N+ membranes following the manufacturer's instructions (Wiens et al., 1998). Hybridization was performed with the complete silicatein probe from *G. cydonium* (*GCSILICA*). Northern blot signals were quantified using the chemiluminescence procedure (Stanley and Kricka, 1990) with CDP-Star as substrate. The screen was scanned with a GS-525 Molecular Imager (Bio-Rad, Hercules, CA, USA).

Further analytical methods

. For the quantification of protein the Bradford method (Compton and Jones, 1985; Roti-Quant solution, Roth) was used. The N-terminus of the mature

silicatein was determined after size separation by SDS-PAGE and direct protein sequencing, as described earlier (Pfeifer et al., 1993). Automated aa sequence analysis was performed using a gas-phase protein sequencer (Applied Biosystems; Model 470).

Results

The spicules of *G. cydonium*

The different types of the spicules of *G. cydonium* are arranged in a highly organized pattern within the body of the specimens. Already the first descriptions of the spicules of *G. cydonium* (*Alcyonium primum*) by Donati (1753) (Fig. 1A and B) and Linné (1788) (*Alcyonium cydonium*) identified the zonation of the sponge as well as the two types of spicules, which Donati termed "Stacheln" and "Kügelchen" (Fig. 1A and B). In a cross-section (Figs. 1B, C and 2A), globular specimens which can reach diameters of 10 cm, form a 4–8 mm thick cortex (ectosome) which surrounds the central body. The cortex comprises three regions: (i) the thin ectochrote with numerous oxyasters and fine ectosomal spicules, (ii) the sterrastral layer which is almost totally filled with these microscleres, and (iii) the fibrous layer containing only a few sterrasters (Fig. 2A). The choanosome which follows the subcortical crypts contains masses of large oxeas and triaenes which are oriented concentrically in bundles towards the center of the animal. Fig. 2B shows at a higher magnification a sterraster within the ectochrote zone, together with the fine ectosomal spicules. In addition a sterraster in the fibrous layer, which supports the sterrasters layer, is given together with broken megascleres (Fig. 2C).

The sizes of the sterrasters range between 30 and 75 μm (Fig. 3B) and oxyasters have dimensions of 5–25 μm (Fig. 3A). The megascleres are much longer; the oxeas have a length of 2–4 mm, while the triaenes reach 5 mm (protriaenes [Fig. 2G]) to 6 mm (anatriaenes [Fig. 2F]); their diameters are 20–30 μm.

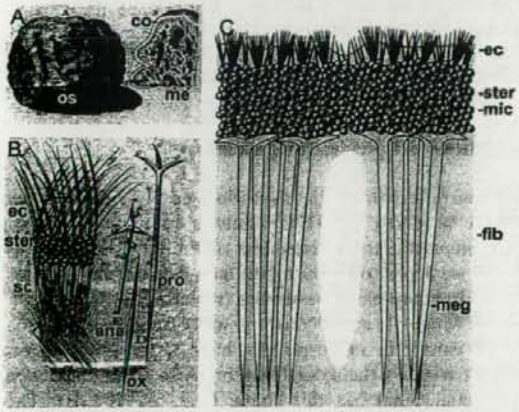

Fig. 1. *Geodia cydonium* (A, B) First description of this species by Donati (1753). At that time the species was termed *Alcyonium primum*. Besides illustrating the total animal (A) with its oscule (os) (left), he gave also a cross-section (right) where he differentiated between the cortex (co) and the central part of the animal, the medulla (me), comprising the aquiferous system. (B) A schematic outline of the arrangement of the spicules in the cortex region with the small spicules ("Stacheln") in the ectochrote at the surface of the specimens (ec), the numerous oxyasters ("Kügelchen"; ster [sterrasters]) and the subcortical crypts (sc) with the large oxeas. At a higher magnification he documented the existing types of megascleres, the anatriaenes (B: ana), the protriaenes (B: pro) and the oxea (B: ox). (C) Schematic outline of the cortical layer of *G. cydonium*: the ectochrote (ec), the sterraster layer (ster) with the microscleres (mic) and the fibrous (fib) subcortical crypts containing high numbers of large megascleres (meg).

Morphology of microscleres (sterrasters and oxyasters)

The sterrasters represent polyaxial microscleres, whose axes/rays originate from the center of the spicules. Initially, the sterrasters develop as oxyasters with 150–300 centripetally elongating rays, composed of silica. After reaching a size >5 μm the siliceous axes fuse and form ball-like sterrasters (Figs. 3B and 4A). In the mature stage the ends of the tips have flat, five-pointed structures (Fig. 4B). The immature tips of the sterrasters are spiny and without any ornamentation (Fig. 4C). The tips of the rays are fragile, and where broken, the central canal becomes visible (Fig. 4C). If the sterrasters grow further, the tips start to form small ramifications (intermediate stage; Fig. 4D). At a higher magnification the axial canals, existing in the ends of the rays become visible (Fig. 4E). Those rays in the center, which have fused together to a solid ball-like body leave the axial canals still open (Fig. 4F). In cross-sections it can be seen that the center of the asters is solid and breaks during the cutting of a sample, while in the periphery of the asters the rays are separated (Fig. 4G) and can be visualized individually (Fig. 4H). The siliceous shell around the axial canals of the rays breaks to typical lumps (Fig. 4G and H).

The thorned oxyasters (Fig. 3A) are much smaller than the sterrasters (Fig. 3B) and comprise regularly eight rays. The tips of the silicified rays of the globular sterrasters are arranged around a central dent (Fig. 3B–D). The origin or the function of this cavity is not known. Microscopic inspection suggests that these

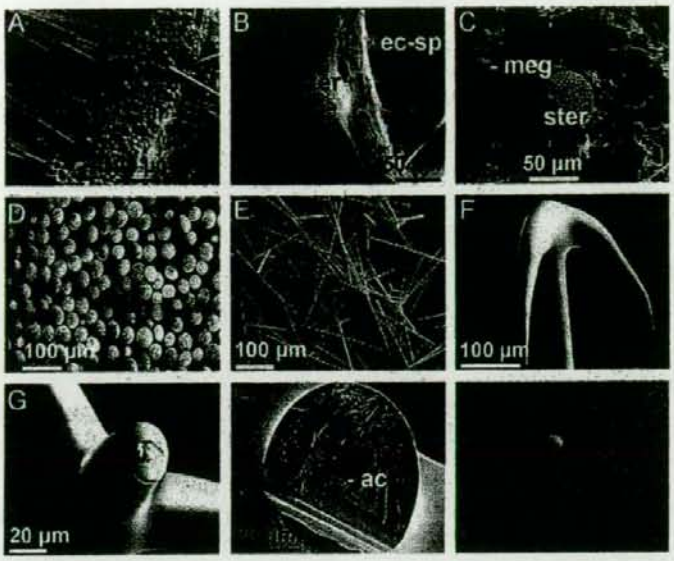

Fig. 2. Sterrasters in different regions within the cortex: (A) a cross-section through the cortex demonstrates its zonation. The surface is formed by the ectochrote (ec) with its numerous sterrasters (ster) and fine ectosomal spicules. This layer is supported by a zone composed almost exclusively of sterrasters (ster). This microsclere layer is finally followed by the fibrous (fib) subcortical crypts containing high numbers of large oxeas and triaenes. (B) At higher magnification the fine ectosomal spicules (ec-sp) can be visualized together with a sterraster (ster). (C) One sterraster, in the fibrous layer that is surrounded by megascleres (meg). (D, E) Purified fractions of microscleres (D) and megascleres (E). (F) The tip of a megasclere (anatriaene). (H, I) The megascleres (here shown for the protriaenes) contain in their protrusions axial canals (ac) which has a triangular form. SEM analyses.

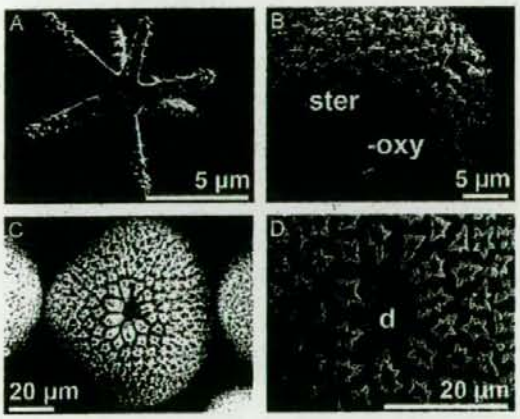

Fig. 3. SEM analyses of the two types of microscleres: (A) the small oxyaster displays eight rays around which silica is appositionally deposited. (B) One sterraster (ster) which is associated with an oxyaster (oxy). (C) One sterraster, showing that the tips of the silicified rays are arranged around a central dent. (D) At a higher magnification the central dent (d) is visible which is surrounded by mature tips.

dents might provide the socket for the megascleres which are closely associated with them in the fibrous layer, supporting the sterrastral layer (Figs. 1C and 2A).

Synthesis of spicules (megascleres)

Even after thorough inspection no clear-cut images could be taken by TEM analysis in tissue from *G. cydonium*, due to the hardness of the bio-silica. Therefore, we have to restrict our data to the megascleres only. In comprehensive studies (reviewed in: Uriz et al., 2003; Müller et al., 2006a) it is well established that the axial canals in demosponges have a triangular form which harbors the axial filament. Also in *G. cydonium* the axial canal has this shape (Fig. 5A and B). The mature megascleres, with a diameter of approximately 15 µm, exist in the mesohyl, the bulky extracellular space associated, but not attached with cells, the sclerocytes (Fig. 5C). In the center of the silica mantel (broken to lumps) lies the ≈1 µm thick axial filament. Around these spicules are collagen fibrils which follow the shape of the spicules (Fig. 5D). Higher magnification shows that the collagen fibrils are twisted towards the surface of the silica mantel of the spicules (Fig. 5E). Occasionally the collagen fibrils appear to protrude into the silica lumps (Fig. 5F). As described for the spicule formation in *S. domuncula* (Müller et al., 2005b), the axial filament is formed intracellularly in sclerocytes where also the first silica layer is formed (Fig. 5G and H). These sclerocytes are surrounded by a net of collagen fibrils. If released into the extracellular space the spicules are

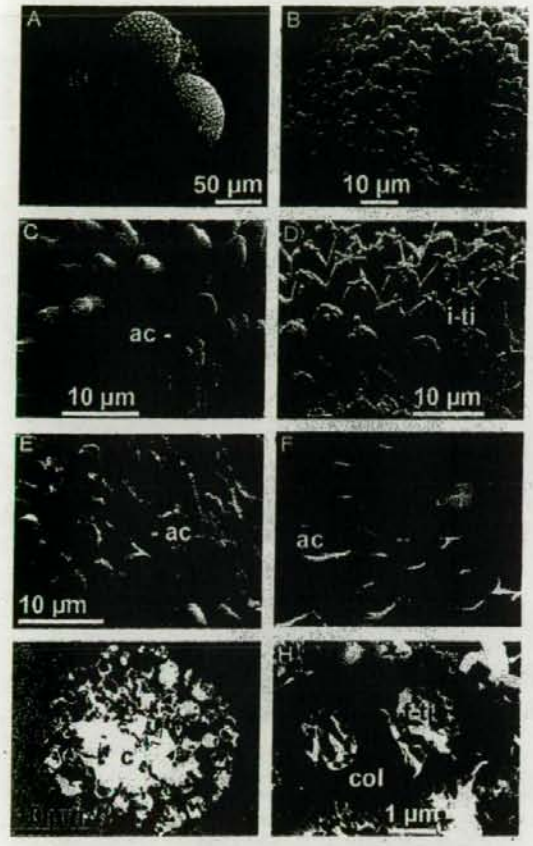

Fig. 4. Morphology of sterrasters; SEM (A–F) and TEM (G, H) analyses. (A) Sterrasters. (B) Mature sterrasters, displaying the flat, five-pointed structures at the ends of the tips (f-ti). (C) Immature tips of the spiny sterrasters (s-ti) without any ornamentation; where broken the axial canals (ac) in the spines are visible. (D) Intermediate developmental stage of the sterrasters with the small ramifications on the tips of the rays (i-ti). (E) Broken tips which comprise one axial canal (ac). (F) In the center of the ball-like sterrasters the silica shells composing the rays have fused and leave the axial canals open (ac). (G) Cross-section through tissue with one embedded sterraster. In the center (c) of the microsclere the silica is broken and the lumps are removed; on the surface, rays (ra) are seen. (H) Higher magnification of the outer region of the aster with terminally developed tips (f-ti); these are surrounded by collagen fibrils (col).

surround by collagen fibrils in longitudinal and traverse direction (Fig. 5I and J). This collagen net covers also the surface tips of the ball-like sterrasters (Fig. 4H). The axial canal remains open even after completion of the spicules and continues to harbor the triangular axial filament (Fig. 5K).

The megascleres, as shown here for the anatriaenes, comprise not only in the long axial part of the spicules an axial canal, but have an axial canal also in the protrusions/hooks (Fig. 2G–I). The form of this "diverging" axial canal is – like in other megascleres – also triangular (Uriz et al., 2003).

Dissolution of the silica shell from the organic filaments

Cleaned spicules were treated with HF, as described under "Materials and methods" to set the axial filament free. After this treatment the proteinaceous axial filaments of the megascleres could be identified by staining with Coomassie brilliant blue (data not shown). They have the same rod-like appearance as documented for *S. domuncula* (Müller et al., 2006b). An SEM image of the megasclere axial filament from *G. cydonium* is presented in Fig. 5L. To determine if also in the axial canals of the microscleres axial filaments are present, a stepwise dissolution of the silica material of the sterrasters was performed. After transfer of the sterrasters into buffered HF, no proteinaceous material can be stained with Coomassie brilliant blue (Fig. 6A). However, already after 5 min the first axial filaments were exposed and immediately stained blue (Fig. 6B). Most asters lost their silica after a 15-min incubation period (Fig. 6C). The light microscopic data could be confirmed by SEM analysis. After a 3-min dissolution period the silica shell around the asters started to dissolve (Fig. 6D), while the first complete fibrillar matrix could be visualized after a 30-min treatment with HF (Fig. 6E). The tips of the filaments are swollen to blebs (Fig. 6F).

Separation of microscleres from megascleres

The data of the preceding section show that the two different types of scleres in *G. cydonium* contain an organic axial filament. In order to determine specifically the proteinaceous composition of the axial filaments the microscleres were separated from the megascleres. Microscopic inspection revealed that both, the microsclere (Fig. 2D) and the megasclere fractions (Fig. 2E) used for further analysis were almost totally pure. From these samples axial filaments were prepared.

Protein analysis of the axial filament

The axial filament protein samples, obtained from the microsclere and the megasclere fractions were subjected to SDS-PAGE. This separation revealed different protein patterns in the respective spicule fractions. While the proteins from microscleres showed two main protein bands of apparent sizes of 25 and 60 kDa (Fig. 7A, lane a), the extracts from megascleres have in

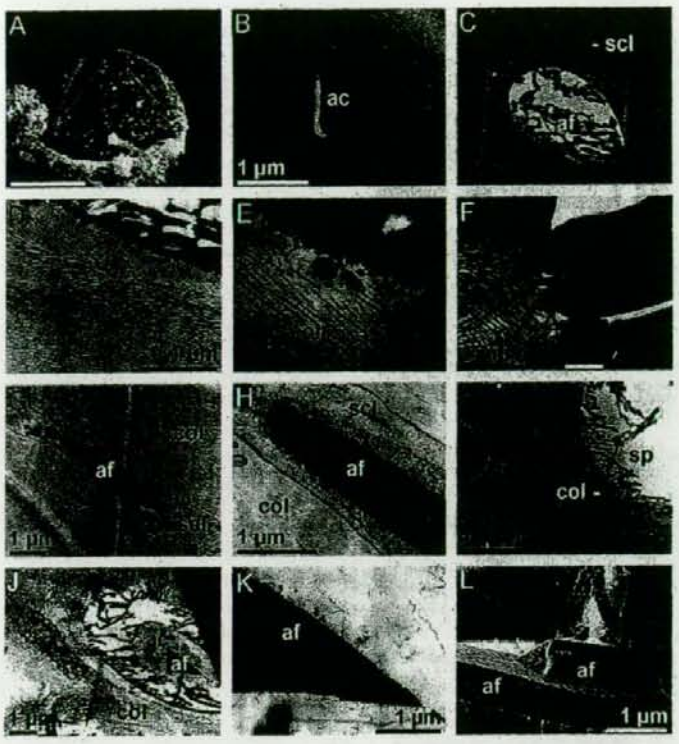

Fig. 5. Megascleres; SEM (A, B and L) and TEM (C–K) analyses. (A) Megasclere of *G. cydonium* and (B) broken megasclere displaying the triangular axial canal (ac). (C) Location of one megasclere in the mesohyl. The oxea is surrounded by a sclerocyte (scl) and harbors in the center an axial filament (af). (D–F) A corset composed of collagen fibrils (col) surrounds the spicules. More distantly the collagen fibrils follow the shape of the spicules (D), while in closer vicinity the collagen fibrils protrude almost into the silica lumps (F). (G, H) The synthesis of the spicules starts intracellularly in a sclerocyte (scl) with the formation of an axial filament (af). The cells are surrounded by collagen (col). (I) The megascleres are subsequently extruded into the extracellular space. (J, K) In a mature oxea the triangular axial filament (af) remains in the axial canal (ac). (L) Axial filaments, obtained from oxea, with their triangular shapes.

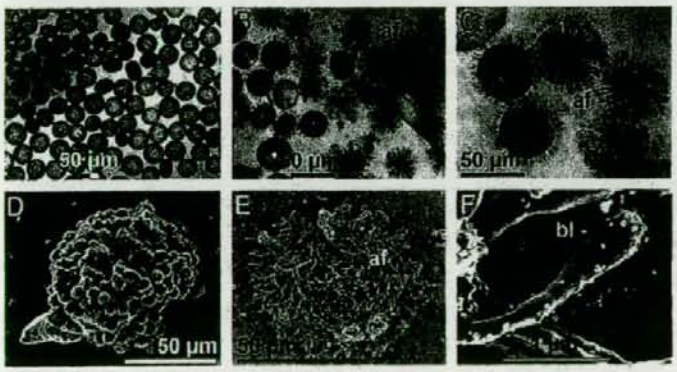

Fig. 6. Dissolution of silica around the microscleres with hydrofluoric acid. (A–C) The light optical micrographs were taken progressively after 1 min (A), 5 min (B) or 15 min (C). Simultaneously with the liberation of the axial filaments, these fibrils were stained blue, with Coomassie brilliant blue. (D–F) Electron microscopic images (SEM). The spicules were treated with hydrofluoric acid for 3 min (D) or 30 min (E, F). At a higher magnification swollen tips/blebs (bl) of the axial filaments are seen.

addition to the 25-kDa polypeptide, two further major protein bands with sizes of 27 and 24 kDa (Fig. 7A, lane b). The same protein pattern was seen if the gels were stained with SYPRO Ruby protein gel stain, as described (Müller et al., 2005b); data not shown. Western blot analyses were performed to identify the nature of these protein bands. At first, polyclonal anti-silicatein antibodies (PoAb-aSilic) were applied which reacted only with the 25-kDa molecule in the microsclere extract (Fig. 7B, lane a). In contrast, among the proteins from the megascleres, the polypeptides with sizes of 27 and 24 kDa were found to cross-react (Fig. 7B, lane b). Based on a previous preliminary nomenclature (Shimizu et al., 1998), the molecules cross-reacting with PoAb-aSilic were designated as silicatein-α (27 kDa), silicatein-α/β (25 kDa) and silicatein-γ (24 kDa). Considering that – until now – no gene, coding for silicatein-γ has been identified in *G. cydonium* and also not in *T. aurantium* and due to the high similarity of the cloned 25-kDa silicatein to the silicatein-α group (see below), this new 25 kDa silicatein from *G. cydonium* was named silicatein-α/β (Fig. 7B, lanes a and b).

A second polyclonal antibody, raised against the sponge protein collagen, was applied in the Western blot studies. These antibodies strongly cross-react with the 60-kDa protein, existing in extracts from microscleres and megascleres (Fig. 7C, lanes a and b). Controls, both for the Western blot studies with the antibodies against silicatein and collagen were performed with pre-adsorbed PoAb-aSilic or PoAb-aCol samples; with these samples no cross-reaction with any protein on the blot was seen (not shown).

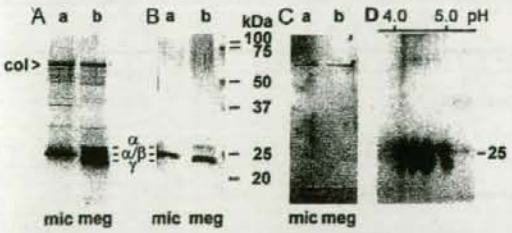

Fig. 7. Analysis of proteins in spicule extracts from microscleres (mic; lanes a) or megascleres (meg; lanes b). (A) The protein samples were subjected to SDS-PAGE and stained. (B) The size separated proteins were transferred to membranes and reacted with polyclonal anti-silicatein antibodies. The different isoforms of silicatein (-α, -α/β and -γ) are marked. (C) In a separate series of experiments the membranes were reacted with anti-collagen antibodies. The protein species which reacted with anti-collagen antibodies is indicated (col). (D) Analysis of the proteins in the extract from megascleres by two-dimensional gel electrophoresis (first isoelectric focusing and then size separation). The electrophoresis was conducted as described under "Materials and methods". The size of the silicateins is marked (25 kDa).

In order to clarify whether silicatein-α/β from the axial filament in microscleres undergoes post-translational modification 2D gel electrophoresis (isoelectric focusing – size separation) was performed (Fig. 7D). It became clear, that the 25-kDa silicatein-α/β molecules exist with four different isoelectric points (p*I*). The first spot can be visualized at a pH of 5.0, while the following three forms have a p*I* of 4.7, 4.4 and 4.1. Based on this study we suggest that the silicateins from the microscleres of *G. cydonium* undergo phosphorylation (Fig. 7D). A p*I* shift of approximately 0.3 pH units results per one suggested additional phosphorylation step, which is in accordance with findings from other phospho-proteins (Towbin et al., 2001). In order to demonstrate experimentally that the silicateins really undergo phosphorylation and not any other modification which results in a change of the p*I* value, the "PhosphoProbe assay" (Pierce Chemicals, Rockford, IL, USA) as well as the periodic acid-Schiff (PAS) staining procedure (Glycoprotein Detection Kit; Sigma) were applied. While positive signals were seen in the phospho-protein assay, no spots were detected after PAS staining (data not shown).

Identification of the silicatein from axial filaments of microscleres: cloning of the gene

The cDNA encoding the *G. cydonium* silicatein (*GCSILICA*) was obtained as described under "Materials and methods" using a degenerate primer set designed against conserved regions in silicatein-α cDNAs. Northern blot analysis revealed a transcript size of ~1.3 kb (not showed). The open reading frame (ORF), between nt_{40-42} and $nt_{1042-1044(stop)}$, codes for a 334 aa long polypeptide (SILICAa/b_GEOCY) with a predicted size of 36,332 and a p*I* of 5.44 (Fig. 8A). Like the related silicateins from *S. domuncula* or *T. aurantium*, also the *G. cydonium* silicatein comprises a short signal peptide, with 20 amino acids. In addition a cleavage site between the propeptide and the mature peptide can be predicted; it is located between aa_{116} and aa_{117}. The deduced size of the mature silicatein, with its 218 aa is 23,190; the p*I* has been computed with 5.04.

The catalytic triad amino acids characteristic of silicateins, Ser (aa_{142}), His (aa_{281}) and Asn (aa_{300}), are present at positions which match those described for the other silicateins (Cha et al., 1999; Krasko et al., 2000) (Fig. 8A). Likewise, the serine cluster (Shimizu et al., 1998) is found between aa_{258} and aa_{277}; in contrast to other hitherto analyzed silicateins the *G. cydonium* protein comprises a longer (9 Ser) serine cluster.

A phylogenetic analysis of the new *G. cydonium* silicatein was performed together with other related sequences within the cathepsin/cysteine protease family (Fig. 8B). The *G. cydonium* silicatein falls within the

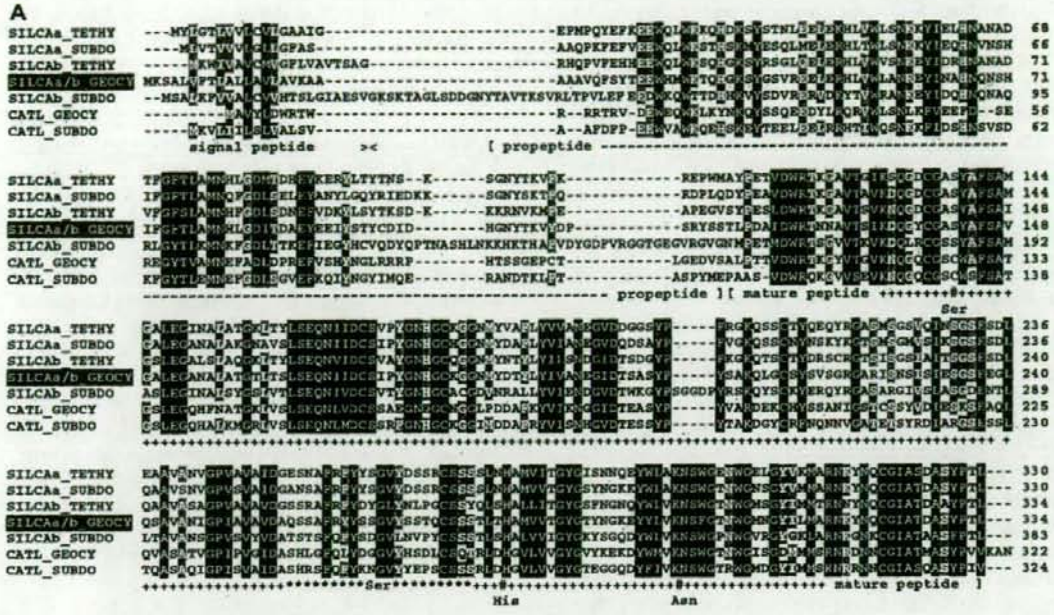
A
SILCAa_TETHY
SILCAa_SUBDO
SILCAb_TETHY
SILCAa/b_GEOCY
SILCAb_SUBDO
CATL_GEOCY
CATL_SUBDO
signal peptide
propeptide
mature peptide
Ser
His
Asn

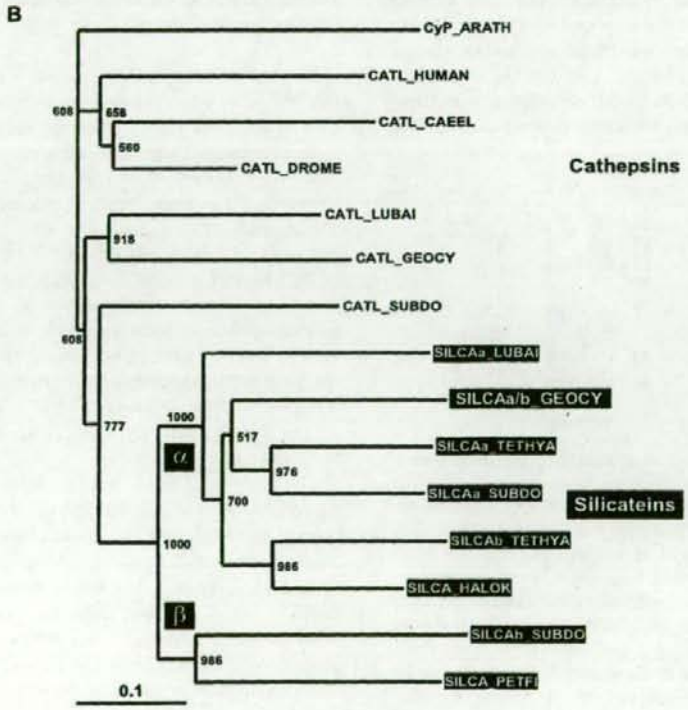
B
CyP_ARATH
CATL_HUMAN
CATL_CAEEL
CATL_DROME
CATL_LUBAI
CATL_GEOCY
CATL_SUBDO
SILCAa_LUBAI
SILCAa/b_GEOCY
SILCAa_TETHYA
SILCAa_SUBDO
SILCAb_TETHYA
SILCA_HALOK
SILCAb_SUBDO
SILCA_PETFL
Cathepsins
Silicateins
α
β
0.1

group of the silicateins-α, and was therefore termed SILCAa/b_GEOCY. The additional index "b" was chosen, since the size of the other known silicatein-α proteins is approximately 2–3 kDa higher. As seen in the rooted tree (Fig. 8B) the distinctions of the silicateins-α from the silicateins-β is not statistically significant, since the silicatein-β from *T. aurantium* groups to other silicateins-α; only the β-isoforms from *S. domuncula* and *Petrosia ficiformis* are distinctly separated. Separated from the silicateins are the cathepsins L from metazoa, with those from the sponges *S. domuncula* and *G. cydonium*, from human, *Drosophila melanogaster* and *Caenorhabditis elegans* as examples (Fig. 8B). Other cysteine proteases, e.g. those from *Arabidopsis thaliana* are not in the group of metazoan silicateins and cathepsins L.

Identification of the silicatein from axial filaments of microscleres: amino acid sequencing

The N-terminus of the PAGE-purified *G. cydonium* silicatein-α/β from microscleres (the 25-kDa polypeptide) was sequenced; and the first 10 aa, TLPDAIDWRT, were found to be identical with the aa moieties, aa_1–aa_{10}, in the predicted mature silicatein-α/β deduced from the cDNA.

Discussion

The basic morphological descriptions of the spicules from *G. cydonium* go back to Donati (1753). This author already described the zonation of the animals with the cortical layer on the surface (later termed ectosome), followed by the sterrastral layer which surrounds the central medulla, the main part of the body. Since then – due to the technological advancement – a more detailed analysis of the morphology was achieved (see Uriz, 2002). Like in any other siliceous sponge, also in *G. cydonium*, the inorganic material from which the skeletal elements are formed is Si-dioxide.

The spicules are formed intracellularly; during this initial formation fibers are involved which – however – never become included in the axial filament (Müller et al., 2005b, 2006a). During the maturation process the homogeneous proteinaceous material within the axial canal condenses and forms the more compact axial filament (Müller et al., 2005b). The major molecule which facilitates/mediates the formation of the siliceous spicules is the enzyme silicatein (see Introduction). Until now the focus in the understanding of the morphological and biochemical basis of spicule formation concentrated on the development and morphology of larger megascleres in demosponges, with *T. aurantium* (reviewed in Weaver and Morse, 2003) and *S. domuncula* (reviewed in Müller et al., 2006a) as the model sponges. Silicatein molecules form the organic axial filament, which exists in the axial canal of the spicules. The axial canal is one of the characteristics seen in all megascleres and also – as shown here for the first time – in the smaller microscleres. Strong evidence has been presented that it is the silicatein which synthesizes/condensates bio-silica from monomeric *ortho*-silicate (Cha et al., 1999; Krasko et al., 2000). Surprising was the finding that the freshwater sponges, e.g. *Lubomirskia baicalensis*, comprise a higher silicatein polymorphism [this species contains over five different silicatein genes (Müller et al., 2007a)] compared to marine sponges, from which only two different isoforms have been described (Cha et al., 1999; Krasko et al., 2000; Schröder et al., 2007). Biochemical studies revealed that in all hitherto studied axial filaments of megascleres at least two silicatein isoforms exist (Shimizu et al., 1998; Müller et al., 2005b Schröder et al., 2006). Based on these findings a hypothesis on the packaging of the silicateins within the axial filament has been formulated (Croce et al., 2004; Murr and Morse, 2005). After the introduction of a non-harsh procedure to isolate the silicatein from spicules it became possible to suggest that these molecules assemble in a fractal-like manner (Müller et al., 2007b).

The amazing intricate species-specific morphology of the spicules of the siliceous sponges is highly enigmatic

Fig. 8. Grouping of the deduced protein sequences of silicateins within the cathepsin/cysteine protease family. (A) The deduced silicatein protein sequence of *Tethya aurantia* [*T. aurantium*] (SILCAa_TETHY; AAD23951) was aligned with the silicateins-α from *S. domuncula* (SILCAa_SUBDO; AJ272013), the silicateins-α/β from *Geodia cydonium* (SILCAa/b_GEOCY; AM500857), and the silicateins-β from *Tethya aurantia* (SILCAb_TETHY; AF098670) and *S. domuncula* (SILCAb_SUBDO; AJ547635.1) as well as with the cathepsin L proteins from *Geodia cydonium* (CATL_GEOCY; Y10527) and *S. domuncula* (CATL_SUBDO; AJ784224). Residues conserved (similar or related with respect to their physico-chemical properties) in all sequences are shown in white on black, and those in at least two sequences in white on gray. The characteristic sites in the sequences, i.e. the catalytic triad amino acids, Ser (#) in silicateins and Cys in cathepsin, as well as His (#) and Asn (#), and the segments of the propeptide and of the mature peptide are marked. Finally, the serine cluster ([*Ser*]) and the cleavage site of the signal peptide are marked (><). (B) A tree was constructed after aligning these sponge proteins with the silicateins-α from the following species *L. baicalensis* (SILCAa_LUBAI; CAH10753), from *Halichondria okadai* (SILCA_HALOK; AB071667), and from *Petrosia ficiformis* (SILCA_PETFI; AY158071), as well as with the cathepsin L proteins from *L. baicalensis* (CATL_LUBAI; CAH10752), and from other metazoa, human (CATL_Human; X12451), *D. melanogaster* (CATL_DROME; S67481) and *C. elegans* (CATL_CAEEL). The cathepsins/cysteine protease from *Arabidopsis thaliana* (CyP_ARATH; BAB08269.1) has been used as an outgroup.

(Arndt, 1935), a fact which indicates that the form, size and shape of the spicules are determined genetically. However, the process(es) by which – especially in the extracellular space – these spicules are shaped are not yet understood. Therefore, we have chosen a demosponge, *G. cydonium*, which comprises two types of spicules, megascleres (with the two types of oxeas, the protriaenes and the anatriaenes) and microscleres (sterrasters and oxyasters). Both types of spicules have a filigree morphology. The oxeas have one axis (monactinal); in the protriaenes the hooks at one end are directed forward, while the hooks of the anatriaenes are directed backward. In the present study it is demonstrated that the formation of the megascleres in *G. cydonium* starts also intracellularly. The maximal size of the immature spicules in the synthesizing sclerocytes was determined with 10 μm, approximately the same size as for the megascleres in *S. domuncula* (Müller et al., 2006a). The final morphology of the megascleres is trimmed extracellularly to the 2–4 mm long spicules. Extracellularly the spicules are not intimately attached to cells but tightly surrounded by a collagen corset (Eckert et al., 2006).

Here we now show that also the protrusions/hooks of the *G. cydonium* megascleres comprise an axial canal which very likely harbors an axial filament. Both canals, those which run along the longitudinal axis as well as those existing in the "diverging" hooks have a triangular shape. The axial filaments isolated from the megascleres of *G. cydonium* have likewise a triangular shape. In contrast the canals which are seen in the microscleres are almost round. Also in lithistid demosponges the axial canals of the microscleres (desma) are round (Pisera, 2003). This observation was a first hint that major component(s) of the axial filaments in microscleres are different from those existing in megascleres. The morphology of microscleres is much more diverse and more structured. As known since Evans (1900) and Minchin (1909) the development of the microscleres starts intracellularly, while the final synthesis of the asters occurs extracellularly (shown here). In *G. cydonium* the asters are composed of a multitude of silica rays; the oxyasters are composed of eight rays, while the sterrasters are constructed from 150 to 300 centripetally elongating silica rays. It is remarkable that the silica rays are not smooth but highly ornamented, especially at the tips of the mature asters. The tips of the silica rays mature from spines without any ornamentation (immature), via one to five small ramifications (intermediate stage) to tips comprising flat, five-pointed structures (mature). Besides the modifications at the tips of the silica rays also modifications in the more central part of the asters occur. The rays fuse to solid ball-like structures which are traversed by the axial canals, initially forming the rays.

Based on the high species-specific polymorphism of the microsclere morphology, which can be considered to be more complex than in megascleres (Schulze and von Lendenfeld, 1889), it had been expected that also the number of silicatein isoforms might be higher in these skeletal elements. To be able to distinguish between the protein components in the microscleres and the megascleres, the two types of spicules were separated. Unexpectedly the protein composition of the microscleres was less divers than that of megascleres. While three isoforms of silicatein could be identified in megascleres having apparent sizes of 27 kDa (silicatein-α), 25 kDa (silicatein-α/β) and 24 kDa (silicatein-γ), only one silicatein isoform, likely to be silicatein-α/β (25 kDa) could be found in microscleres. In order to rely not only on the sizes of the proteins, which fit very well with the published *S. domuncula* polypeptides (Müller et al., 2005b), immunoblots were performed. This series of experiments confirmed that the anti-silicatein antibodies cross-reacted with the 27 kDa (silicatein-α) and with the 24 kDa (silicatein-γ) isoforms from megascleres and with the 25 kDa (silicatein-α/β) polypeptide in the microscleres. Furthermore, one higher-molecular-weight polypeptide of an apparent size of 60 kDa was detected, which is present in microscleres and also in megascleres. With an antiserum, directed against sponge collagen, the antibodies cross-reacted with the 60-kDa fragment of collagen. By application of SEM and TEM analyses the close association of both the megascleres and the microscleres with collagen could be visualized. In light of published results it is highly likely that the 60-kDa polypeptide reacting with the antibodies, reflects only a collagen fragment; a view which is supported by the work of McBride and Harrington (1965). All hitherto known collagens comprise sizes of >100 kDa (see Bailey, 1971). At present, it might be speculated that during the applied HF treatment a fragmentation of the collagen-like polypeptide has occurred. Already Simpson et al. (1985) raised the question, whether HF treatment of the sponge tissue might destroy the integrity of the proteinaceous meshwork of the sponges. As for megascleres the collagen fibrils also firmly surround the rays of the microscleres, suggesting that they are involved in the silicatein-mediated synthesis/condensation of the bio-silica mantel. Like the silicateins from the megascleres (Müller et al., 2005a), also the 25-kDa (silicatein-α/β) undergoes at least three phosphorylation steps. The different p*I* values of the phosphorylated silicateins have been determined to be 4.7, 4.4 and 4.1; values which are characteristic of the silicateins from the *S. domuncula* megascleres (Müller et al., 2005a).

In order to identify the gene encoding the silicatein-α/β, the corresponding cDNA was isolated using PCR technique. As in other silicateins, also the silicatein-α/β has a predicted cleavage site, not only for the removal of

the signal peptide but also for the cleavage of the propeptide from the mature silicatein. Furthermore, the characteristic catalytic triad Ser-His-Asn exists, which had been described as crucial for the enzymatic function of silicateins (Zhou et al., 1999). This triad differs in one amino acid from the one in cathepsins [Cys-His-Asn] (Shimizu et al., 1998). By terminal sequencing of the N-terminal amino acids of the isolated protein, the identity between the 25-kDa (silicatein-α/β) molecule from microscleres and the protein deduced from the cDNA was confirmed. The phylogenetic analysis of the silicatein-α/β revealed that it groups to the class of α-silicateins. A final decision about the grouping of the silicateins, especially of silicatein-α/β, in *G. cydonium* in comparison to the silicatein-α and -β will be studied next by sequencing the respective coding genes. Nevertheless, the major outcome of this study is the observation that the axial filaments of the microscleres differ strongly from the one of the megascleres.

In conclusion, the results summarized in the present work provide – for the first time – experimental evidence on the different composition of the silicateins in microscleres compared to megascleres in a demosponge in general and for these scleres in one given species. In view of earlier assumptions, silicatein to be a molecule involved in morphogenesis of spicules (megascleres in *S. domuncula*), especially in the extracellular space (Müller et al., submitted for publication), the presented data might indicate that a differential fractal-directed re-assembly between different isoforms and/or different post-translationally modified silicateins is involved in the determination of the morphology of the species-specific spicules. In future, besides comprehensive cloning of the genes, coding for proteins which are involved in the formation of the axial filament in megascleres, a determination of the post-translational modifications of the silicateins in the two types of spicules will be performed.

Acknowledgement

We thank Ms. E. Sehn (Zoological Institute; University of Mainz, Germany) and Mr. M. Plenikowski (Institut für Physiologische Chemie; University of Mainz, Germany) for the valuable technical assistance. This work was supported by grants from the European Commission, the Deutsche Forschungsgemeinschaft, the Bundesministerium für Bildung und Forschung Germany and the International Human Frontier Science Program.

References

Arndt, W., 1935. Die Tierwelt der Nord- und Ostsee, vol. IIIa. Porifera. Akademische Verlagsgesellschaft, Leipzig, pp. IIIa2–IIIa2140.

Bailey, A.J., 1971. Comparative studies on the nature of the cross-links stabilizing the collagen fibres of invertebrates, cyclostomes and elasmobranchs. FEBS Lett. 18, 154–158.

Blumbach, B., Diehl-Seifert, B., Seack, J., Steffen, R., Müller, I.M., Müller, W.E.G., 1999. Cloning and expression of new receptors belonging to the immunoglobulin superfamily from the marine sponge *Geodia cydonium*. Immunogenetics 49, 751–763.

Cha, J.N., Shimizu, K., Zhou, Y., Christianssen, S.C., Chmelka, B.F., Stucky, G.D., Morse, D.E., 1999. Silicatein filaments and subunits from a marine sponge direct the polymerization of silica and silicones in vitro. Proc. Natl. Acad. Sci. USA 96, 361–365.

Coligan, J.E., Dunn, B.M., Speicher, D.W., Wingfield, P.T., 1998. Current Protocols in Protein Science. Wiley, New York, pp. 10.4.1–10.4.36.

Compton, S., Jones, C.G., 1985. Mechanism of dye response and interference in the Bradford protein assay. Anal. Biochem. 151, 369–374.

Croce, G., Frache, A., Milanesio, M., Marchese, L., Causa, M., Viterbo, D., Barbaglia, A., Bolis, V., Bavestrello, G., Cerrano, C., Benatti, U., Pozzolini, M., Giovine, M., Amenitsch, H., 2004. Structural characterization of siliceous spicules from marine sponges. Biophys. J. 86, 526–534.

Dayhoff, M.O., Schwartz, R.M., Orcutt, B.C., 1978. A model of evolutionary change in protein. In: Dayhoff, M.O. (Ed.), Atlas of Protein Sequence and Structure. Nat. Biomed. Research Foundation, Washington, DC, pp. 345–352.

Diehl-Seifert, B., Kurelec, B., Zahn, R.K., Dorn, A., Jerecevic, B., Uhlenbruck, G., Müller, W.E.G., 1985. Attachment of sponge cells to collagen substrata: effect of a collagen assembly factor. J. Cell Sci. 79, 271–285.

Donati, V., 1753. Auszug seiner Natur-Geschichte des Adriatischen Meeres. C.P. Franckens, Halle.

Eckert, C., Schröder, H.C., Brandt, D., Perovic-Ottstadt, S., Müller, W.E.G., 2006. A histochemical and electron microscopic analysis of the spiculogenesis in the demosponge *Suberites domuncula*. J. Histochem. Cytochem. 54, 1031–1040.

Eglin, D., Shafran, K.L., Livage, J., Coradin, T., Perry, C.C., 2006. Comparative study of the influence of several silica precursors on collagen self-assembly and of collagen on 'Si' speciation and condensation. J. Mater. Chem. 16, 4220–4230.

Ehrlich, H., Worch, H., 2007. Collagen, a huge matrix in glass-sponge flexible spicules of the meter-long *Hyalonema sieboldi*. In: In Bäuerlein, E. (Ed.), Handbook of Biomineralization, vol. 1. The Biology of Biominerals Structure Formation. Wiley-VCH, Weinheim, pp. 23–41.

Ehrlich, H., Ereskovskii, A.V., Drozdov, A.L., Krylova, D.D., Hanke, T., Meissner, H., Heinemann, S., Worch, H., 2006. A modern approach to demineralization of spicules in glass sponges (Porifera: Hexactinellida) for the purpose of extraction and examination of the protein matrix. Russ. J. Mar. Sci. 32, 186–193.

Evans, R., 1900. A description of *Ephydatia blembingia* with an account of the formation and structure of the gemmule. Q. J. Microsc. Sci. 44, 71–109.

Exposito, J.Y., Cluzel, C., Garrone, R., Lethias, C., 2002. Evolution of collagens. Anat. Rec. 268, 302–316.

Felsenstein, J., 1993. PHYLIP, ver. 3.5. University of Washington, Seattle.

Garrone, R., 1978. Phylogenesis of Connective Tissue. Karger, Basel.

Garrone, R., Vacelet, J., Pavans de Ceccatty, M., Junqua, S., Robert, L., 1973. Une formation collagène particulière: les filaments des éponges cornies *Ircinia*. Étude ultrastructurale, physico-chimique et biochimique. J. Microsc. 17, 241–260.

Grebenjuk, V.A., Kuusksalu, A., Kelve, M., Schütze, J., Schröder, H.C., Müller, W.E.G., 2002. Induction of (2′–5′)oligoadenylate synthetase in the marine sponges *Suberites domuncula* and *Geodia cydonium* by the bacterial endotoxin lipopolysaccharide. Eur. J. Biochem. 269, 1382–1392.

Imhoff, J.M., Garrone, R., 1983. Solubilization and characterization of *Chondrosia reniformis* sponge collagen. Connect. Tissue Res. 11, 193–197.

Junqua, S., Robert, L., Garrone, R., Pavans de Ceccatty, M., Vacelet, J., 1974. Biochemical and morphological studies on collagens of horny sponges *Ircinia* filaments compared to spongines. Connect. Tissue Res. 2, 193–203.

Krasko, A., Batel, R., Schröder, H.C., Müller, I.M., Müller, W.E.G., 2000. Expression of silicatein and collagen genes in the marine sponge *Suberites domuncula* is controlled by silicate and myotrophin. Eur. J. Biochem. 267, 4878–4887.

Krasko, A., Schröder, H.C., Batel, R., Grebenjuk, V.A., Steffen, R., Müller, I.M., Müller, W.E.G., 2002. Iron induces proliferation and morphogenesis in primmorphs from the marine sponge *Suberites domuncula*. DNA Cell Biol. 21, 67–80.

Kruse, M., Müller, I.M., Müller, W.E.G., 1997. Early evolution of metazoan serine/threonine and tyrosine kinases: identification of selected kinases in marine sponges. Mol. Biol. Evol. 14, 1326–1334.

Kruse, M., Leys, S.P., Müller, I.M., Müller, W.E.G., 1998. Phylogenetic position of the Hexactinellida within the phylum Porifera based on amino acid sequence of the protein kinase C from *Rhabdocalyptus dawsoni*. J. Mol. Evol. 46, 721–728.

Lieberkühn, N., 1856. Zur Entwicklungsgeschichte der Spongillen. Arch. Anat. Physiol., 399–414.

Linné, C., 1788. Systema Naturae; Tomus I, Pars VI. G.E. Beer, Lipsiae.

McBride, O.W., Harrington, W.F., 1965. Evidence for disulfide cross-linkages in an invertebrate collagen. J. Biol. Chem. 240, 4545–4547.

Minchin, E.A., 1909. Sponge-spicules. Erg. Fortschr. Zool. 2, 171–274.

Müller, W.E.G., Borejko, A., Brandt, D., Osinga, R., Ushijima, H., Hamer, B., Krasko, A., Xupeng, C., Müller, I.M., Schröder, H.C., 2005a. Selenium affects biosilica formation in the demosponge *Suberites domuncula*: effect on gene expression and spicule formation. FEBS J. 272, 3838–3852.

Müller, W.E.G., Rothenberger, M., Boreiko, A., Tremel, W., Reiber, A., Schröder, H.C., 2005b. Formation of siliceous spicules in the marine demosponge *Suberites domuncula*. Cell Tissue Res. 321, 285–297.

Müller, W.E.G., Belikov, S.I., Tremel, W., Perry, C.C., Gieskes, W.W.C., Boreiko, A., Schröder, H.C., 2006a. Siliceous spicules in marine demosponges (example *Suberites domuncula*). Micron 37, 107–120.

Müller, W.E.G., Kaluzhnaya, O.V., Belikov, S.I., Rothenberger, M., Schröder, H.C., Reiber, A., Kaandorp, J.A., Manz, B., Mietchen, D., Volke, F., 2006b. Magnetic resonance imaging of the siliceous skeleton of the demosponge *Lubomirskia baicalensis*. J. Struct. Biol. 153, 31–41.

Müller, W.E.G., Wang, X., Belikov, S.I., Tremel, W., Schloßmacher, U., Natoli, A., Brandt, D., Boreiko, A., Tahir, M.N., Müller, I.M., Schröder, H.C., 2006c. Formation of siliceous spicules in demosponges: example *Suberites domuncula*. In: Bäuerlein, E. (Ed.), Handbook of Biomineralization, vol. 1: The Biology of Biominerals Structure Formation. Wiley-VCH, Weinheim, pp. 59–82.

Müller, W.E.G., Wang, X., Belikov, S.I., Wiens, M., Grebenjuk, V.A., Boreiko, A., Schloßmacher, U., Schröder, H.C., 2007a. Silicateins, the major biosilica forming enzymes present in demosponges: protein analysis and phylogenetic relationship. Gene 395, 62–71.

Müller, W.E.G., Boreiko, A., Schloßmacher, U., Wang, X., Tahir, M.N., Tremel, W., Brandt, D., Kaandorp, J.A., Schröder, H.C., 2007b. Fractal-related assembly of the axial filament in the demosponge Suberites domuncula: relevance to biomineralization and the formation of biogenic silica. Biomaterials; in press. doi:10.1016/j.biomaterials.2007.06.030.

Murr, M.M., Morse, D.E., 2005. Fractal intermediates in the self-assembly of silicatein filaments. Proc. Natl. Acad. Sci. USA 102, 11657–11662.

Nicholas, K.B., Nicholas Jr., H.B., 1997. GeneDoc: a tool for editing and annotating multiple sequence alignments. Version 1.1.004. ⟨http://www.nrbsc.org/gfx/genedoc/index.html⟩.

Pancer, Z., Kruse, M., Müller, I., Müller, W.E.G., 1997. On the origin of adhesion receptors of metazoa: cloning of the integrin α subunit cDNA from the sponge *Geodia cydonium*. Mol. Biol. Evol. 14, 391–398.

Pfeifer, K., Haasemann, M., Gamulin, V., Bretting, H., Fahrenholz, F., Müller, W.E.G., 1993. S-type lectins occur also in invertebrates: high conservation of the carbohydrate recognition domain in the lectin genes from the marine sponge *Geodia cydonium*. Glycobiology 3, 179–184.

Pisera, A., 2003. Some aspects of silica deposition in lithistid demosponge desmas. Microsc. Res. Technol. 62, 336–355.

Schmidt, O., 1862. Die Spongien des Adriatischen Meeres. Wilhelm Engelmann, Leipzig.

Schröder, H.C., Krasko, A., Batel, R., Skorokhod, A., Pahler, S., Kruse, M., Müller, I.M., Müller, W.E.G., 2000. Stimulation of protein (collagen) synthesis in sponge cells by a cardiac myotrophin-related molecule from *Suberites domuncula*. FASEB J. 14, 2022–2031.

Schröder, H.C., Boreiko, A., Korzhev, M., Tahir, M.N., Tremel, W., Eckert, C., Ushijima, H., Müller, I.M., Müller, W.E.G., 2006. Co-expression and functional interaction of silicatein with galectin: matrix-guided formation of siliceous spicules in the marine demosponge *Suberites domuncula*. J. Biol. Chem. 281, 12001–12009.

Schröder, H.C., Natalio, F., Shukoor, I., Tremel, W., Schloßmacher, U., Wang, X., Müller, W.E.G., 2007. Apposition of silica lamellae during growth of spicules in the demosponge *Suberites domuncula*: biological/biochemical studies and chemical/biomimetical confirmation. J. Struct. Biol. (E-pub ahead of print).

Schulze, F.E., von Lendenfeld, R., 1889. Die Bezeichnung der Spongiennadeln. Georg Reimer, Berlin.

Sethmann, I., Wörheide, G., 2007. Structure and composition of calcareous sponge spicules: a review and comparison to structurally related biominerals. Micron (E-pub ahead of print).

Shimizu, K., Cha, J., Stucky, G.D., Morse, D.E., 1998. Silicatein alpha: cathepsin L-like protein in sponge biosilica. Proc. Natl. Acad. Sci. USA 95, 6234–6238.

Simpson, T.L., 1984. The Cell Biology of Sponges. Springer, New York.

Simpson, T.L., Langenbruch, P.F., Scalera-Liaci, L., 1985. Silica spicules and axial filaments of the marine sponge *Stelletta grubii* (Porifera, Demospongia). Zoomorphology 105, 375–382.

Sollas, W.J., 1888. Report on the Tetractinellida. In: Wyville Thomson, C. (Ed.), Report on the Scientific Results of the Voyage of HMS Challenger during the Years 1873–76. Eyre & Spottiswoode, London.

Stanley, P.E., Kricka, L.J., 1990. Bioluminescence and Chemiluminescence: Current Status. Wiley, New York.

Swatschek, D., Schatton, W., Kellermann, J., Müller, W.E.G., Kreuter, J., 2002. Marine sponge collagen: isolation, characterisation and effects on the skin parameters surface – pH, moisture and sebum. Eur. J. Pharm. Biopharm. 53, 107–113.

Thompson, J.D., Higgins, D.G., Gibson, T.J., 1994. CLUSTAL W: improving the sensitivity of progressive multiple sequence alignment through sequence weighting, position-specific gap penalties and weight matrix choice. Nucleic Acids Res. 22, 4673–4680.

Towbin, H., Özbey, Ö., Zingel, O., 2001. An immunoblotting method for high-resolution isoelectric focusing of protein isoforms on immobilized pH gradients. Electrophoresis 22, 1887–1893.

Uriz, M.J., 2002. Family Geodiidae, Gray, 1867. In: Hooper, J.N.A., van Soest, R.W.M. (Eds.), Systema Porifera: A Guide to the Classification of Sponges. Kluwer Academic/Plenum Publishers, New York, pp. 134–140.

Uriz, M.J., Turon, X., Becerro, M.A., Agell, G., 2003. Siliceous spicules and skeletal frameworks in sponges: origin, diversity, ultrastructural patterns, and biological functions. Microsc. Res. Tech. 62, 279–299.

von Lendenfeld, R., 1912. Untersuchungen über die Skelettbildungen der Kieselschwämme. Denkschr. Math.-Naturwiss. Klasse Akad. Wien. 88, 693–709.

Weaver, J.C., Morse, D.E., 2003. Molecular biology of demosponge axial filaments and their role in biosilicification. Microsc. Res. Tech. 62, 256–367.

Wiens, M., Koziol, C., Hassanein, H.M.A., Batel, R., Müller, W.E.G., 1998. Expression of the chaperones 14-3-3 and HSP70 induced by PCB 118 (2,3′,4,4′,5-pentachlorobiphenyl) in the marine sponge *Geodia cydonium*. Mar. Ecol. Prog. Ser. 165, 247–257.

Zhou, Y., Shimizu, K., Cha, J.N., Stucky, G.D., Morse, D.E., 1999. Efficient catalysis of polysiloxane synthesis by silicatein α requires specific hydroxyl and imidazole functionalities. Angew. Chem. [Int. Ed.] 38, 780–782.

Available online at www.sciencedirect.com
ScienceDirect
Journal of Structural Biology 161 (2008) 188–203
Journal of Structural Biology
www.elsevier.com/locate/yjsbi

Bioorganic/inorganic hybrid composition of sponge spicules: Matrix of the giant spicules and of the comitalia of the deep sea hexactinellid *Monorhaphis*

Werner E.G. Müller [a,*], Xiaohong Wang [b], Klaus Kropf [a], Hiroshi Ushijima [c], Werner Geurtsen [d], Carsten Eckert [a,e], Muhammad Nawaz Tahir [f], Wolfgang Tremel [f], Alexandra Boreiko [a], Ute Schloßmacher [a], Jinhe Li [g], Heinz C. Schröder [a]

[a] *Institut für Physiologische Chemie, Abteilung Angewandte Molekularbiologie, Universität, Duesbergweg 6, D-55099 Mainz, Germany*
[b] *National Research Center for Geoanalysis, 26 Baiwanzhuang Dajie, CHN-100037 Beijing, PR China*
[c] *Department of Developmental Medical Sciences, Institute of International Health, Graduate School of Medicine, The University of Tokyo, 7-3-1 Hongo, Bunkyo-ku, Tokyo 113-0033, Japan*
[d] *Division of Operative Dentistry, Department of Restorative Dentistry, School of Dentistry, University of Washington, Seattle, WA 98195-7456, USA*
[e] *Museum für Naturkunde, Institut für Systematische Zoologie, Invalidenstraße 43, D-10155 Berlin, Germany*
[f] *Institut für Anorganische Chemie und Analytische Chemie, Universität, Duesbergweg 10-14, D-55099 Mainz, Germany*
[g] *Institute of Oceanology, Chinese Academy of Sciences, 7 Nanhai Road, CHN-266071 Qingdao, PR China*

Received 9 June 2007; received in revised form 16 October 2007; accepted 17 October 2007
Available online 26 October 2007

Abstract

The giant basal spicules of the siliceous sponges *Monorhaphis chuni* and *Monorhaphis intermedia* (Hexactinellida) represent the largest biosilica structures on earth (up to 3 m long). Here we describe the construction (lamellar organization) of these spicules and of the comitalia and highlight their organic matrix in order to understand their mechanical properties. The spicules display three distinct regions built of biosilica: (i) the outer lamellar zone (radius: >300 μm), (ii) the bulky axial cylinder (radius: <75 μm), and (iii) the central axial canal (diameter: <2 μm) with its organic axial filament. The spicules are loosely covered with a collagen net which is regularly perforated by 7–10 μm large holes; the net can be silicified. The silica layers forming the lamellar zone are ≈5 μm thick; the central axial cylinder appears to be composed of almost solid silica which becomes porous after etching with hydrofluoric acid (HF). Dissolution of a complete spicule discloses its complex structure with distinct lamellae in the outer zone (lamellar coating) and a more resistant central part (axial barrel). Rapidly after the release of the organic coating from the lamellar zone the protein layers disintegrate to form irregular clumps/aggregates. In contrast, the proteinaceous axial barrel, hidden in the siliceous axial cylinder, is set up by rope-like filaments. Biochemical analysis revealed that the (dominant) molecule of the lamellar coating is a 27-kDa protein which displays catalytic, proteolytic activity. High resolution electron microscopic analysis showed that this protein is arranged within the lamellae and stabilizes these surfaces by palisade-like pillars. The mechanical behavior of the spicules was analyzed by a 3-point bending assay, coupled with scanning electron microscopy. The load-extension curve of the spicule shows a biphasic breakage/cracking pattern. The outer lamellar zone cracks in several distinct steps showing high resistance in concert with comparably low elasticity, while the axial cylinder breaks with high elasticity and lower stiffness. The complex bioorganic/inorganic hybrid composition and structure of the *Monorhaphis* spicules might provide the blueprint for the synthesis of bio-inspired material, with unusual mechanical properties (strength, stiffness) without losing the exceptional properties of optical transmission.

Keywords: Hybrid composite material; Sponges; *Monorhaphis*; Spicules; Elasticity; Silicatein

* Corresponding author. Tel.: +49 6131 39 25910; fax: +49 6131 39 25243.
E-mail address: wmueller@uni-mainz.de (W.E.G. Müller).
URL: http://www.biotecmarin.de/ (W.E.G. Müller).

1047-8477/$ - see front matter © 2007 Elsevier Inc. All rights reserved.
doi:10.1016/j.jsb.2007.10.009

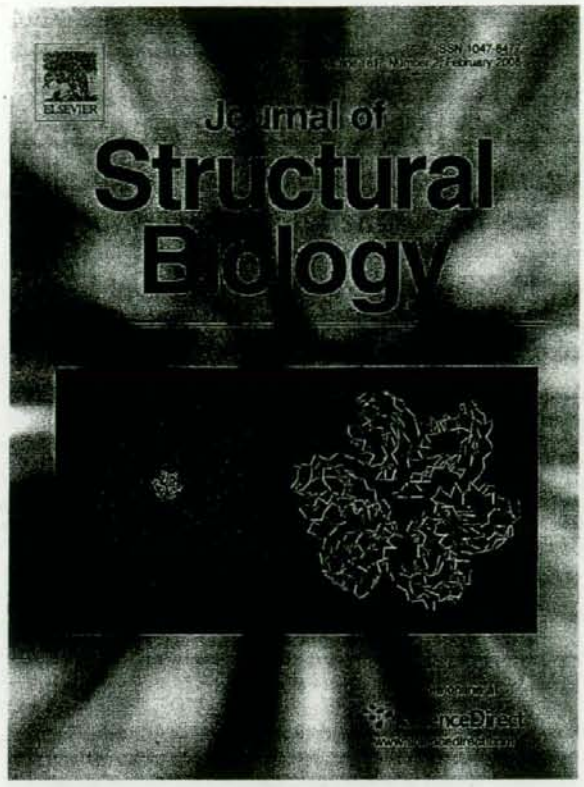

1. Introduction

The earth's surface is composed of more than 55% silicon and oxygen. Silicon is present mainly as silica and silicates. In the inorganic natural state it is found primarily as anhydrous quartz, cristobalite and tridymite; moreover, in soils and hot-springs silica exists as amorphous opal-A and also as rigid/flexible biological material, e.g. bio-silica, and combines the properties of strength and stiffness with toughness (Mayer, 2005). The toughness of rigid biological skeletal material, irrespective if made of calcium or silica minerals, is in the first place caused by the lamellar organization of the inorganic matrix, as seen in nacre of mollusk shells (calcareous material) or in spicules in sponges (phylum Porifera) of the classes of Demospongiae and Hexactinellida (siliceous biomineral) (reviewed in Mayer, 2005). The strength of siliceous skeletal spicules has been studied in great detail in the hexactinellid sponge *Euplectella aspergillum* (Aizenberg et al., 2005; Weaver et al., 2007; Woesz et al., 2006). The spicules of hexactinellid sponges gained additional attention because of their fiber-optic properties; they can function as single-mode, few-mode, or multimode fibers, with spines serving as illumination points along the spicule shaft (Aizenberg et al., 2004; Müller et al., 2006b; Wang et al., 2007).

For our biochemical, optical, and biomechanical studies with spicules from Hexactinellida we have used the giant basal spicules (and the comitalia) of glass sponges, *Hyalonema sieboldi* (Müller et al., 2006b) and two other closely related species, *Monorhaphis chuni* and *Monorhaphis intermedia* (Müller et al., 2007a; Wang et al., 2007). These species are grouped to the order of Amphidiscoida, while the hexactinellid *E. aspergillum* that has been primarily studied by Aizenberg and colleagues (2005) and Weaver and colleagues (2007) belongs to the order Hexactinosida (Tabachnick, 2002; Reiswig, 2006). The most outstanding feature of the spicules from *Monorhaphis* is their size; the giant basal spicules are with up to 3 m (diameter of up to 8 mm) the longest/largest bio-silica structures on earth (Schulze, 1925). The morphology of these giant basal spicules has earlier been thoroughly described (Schultze, 1860, 1904, 1925; Levi et al., 1989). Cross sections of the giant spicule of *Monorhaphis* allow the distinction of three zones; (i) the outer lamellar zone (radius: >300 μm), (ii) the bulky axial cylinder (radius: <75 μm), and (iii) the central axial canal (diameter: <2 μm) that surrounds the organic axial filament (Müller et al., 2007a; Wang et al., 2007). The outer lamellar zone is composed of 300–500 lamellae that are concentrically arranged and are each 3–8 μm thick. Related to these giant basal spicules, with respect to their structure, are the comitalia which reach sizes of 60 mm (length) and 0.5 mm (diameter).

An outstanding feature of siliceous spicules, from both Demospongiae and Hexactinellida, is the formation of the silica shell around the axial canal/axial filament. The group of Morse (Shimizu et al., 1998; Cha et al., 1999) described that the major protein of the axial filament of the demosponge *Tethya aurantium* is an enzyme which they termed silicatein, that mediates polymerization/condensation of ortho-silicate to polymeric (bio)silicate (Cha et al., 1999). Shortly after, this enzyme was also identified in the demosponge *Suberites domuncula* (Krasko et al., 2000). The silicateins belong to the cathepsin L-proteinase family, and are distinguished from them by one amino acid in the catalytic center (catalytic triad Ser-His-Asn (in silicatein) and Cys-His-Asn (in cathepsins)) (Cha et al., 1999; Krasko et al., 2000; Müller et al., 2007c). It is well established that cathepsins can be effectively inhibited by E-64 (L-*trans*-epoxysuccinyl-leucylamido(4-guanidino)butane) through binding to the active sites of the enzymes (Barrett et al., 1982, 2002).

For the demosponge *S. domuncula* a detailed biochemical and cytochemical analysis of the synthesis of the siliceous spicules was established (reviewed in Müller et al., 2006a, 2007b). In brief, growth of the spicules starts intracellularly (Müller et al., 2005). After having reached a length of about 8 μm, the primordial spicules are extruded from the cells and reach in the extracellular space their final forms by longitudinal and lamellar thickening growth. The size-increase of the spicules occurs by lamellar apposition of silica layers, which are separated by sheets of organic matrices formed of galectin (Schröder et al., 2006). Despite the attractiveness of biosilica for biotechnological (reviewed in Morse, 2001; Patwardhan et al., 2005; Müller et al., 2007b) and biomimetical applications (Wang and Wang, 2006) and despite the fact that only in sponges is biosilica formed via an enzyme, no detailed analyses of the proteinaceous components of spicules from hexactinellids have yet been undertaken (see Leys et al., 2007). The spicules of most hexactinellids are larger and more luxuriously architectured than those in demosponges (Tabachnick, 2002). Very likely, also in hexactinellids growth of spicules starts from an axial filament (Hartman, 1983 and reviewed in Leys et al., 2007), around which bio-silica with the general formula of $SiO_2 \bullet nH_2O$ ($n = 0.3$) is formed (Sandford, 2003).

From studies with *Monorhaphis*, Levi and coworkers (1989) suggested that the layered structure of the spicules has a "beneficial" effect on the mechanical properties of the spicules. The concept of natural composite material in rigid biological systems was fundamentally outlined by Mayer (2005). The organic phase controls energy dissipation especially in systems that are interspersed by very thin organic layers. In continuation of this topic Mayer et al. (2005) proposed from their load–displacement studies that in *Euplectella* breakages of spicules follow a telescope-like pattern.

While the first genes from a hexactinellid sponge, *Rhabdocalyptus dawsoni*, encoding proteins (serine/threonine kinases) had been identified already in 1998 (Kruse et al., 1998), first analyses of proteins in spicules have been published only recently. For these studies giant basal spicules from *Monorhaphis* were used because of their large size and their morphology. These spicules contain one protein of a size of around 25/27 kDa and, in addition, higher

molecular weight protein(s) (>60 kDa) (Müller et al., 2007a; Wang et al., 2007). It could be demonstrated that *Monorhaphis* spicules contain two molecules, which have related counterparts in demosponges; a lectin (Schröder et al., 2006) and a silicatein-like protein (reviewed in Wang et al., 2007). Therefore we proposed that the lamellar growth of *Monorhaphis* spicules proceeds by appositional lamellar growth involving very likely silicatein-like protein(s) and lectin (Müller et al., 2007a; Wang et al., 2007). The outer surfaces of the spicules are covered by a collagen net as visualized electron microscopically (Müller et al., 2007a).

In the present study we demonstrate that the proteinaceous matrix of the *Monorhaphis* spicules (the giant basal spicules and the comitalia) is not evenly distributed throughout the inorganic shell around the axial canal. In fact, morphological/structural zones can be distinguished; the axial cylinder and the lamellar zone. Earlier we described the morphology of the giant basal spicules of *Monorhaphis* (Müller et al., 2007b). Now we show, that the layers setting up the lamellar zone are composed (exclusively) of one protein (size: 27 kDa); based on its binding property to labeled E-64 the 27-kDa molecule can be characterized as a protease, a (silicatein-related) polypeptide. Finally, the surface of the spicules is enveloped by a collagen net.

By load–displacement studies it became also possible to correlate the pattern of fractures within the spicules with the organization of the lamellar zone and the axial cylinder; both areas are characterized by different bioorganic/inorganic hybrid compositions.

2. Materials and methods

2.1. Materials

Casein and Coomassie Brilliant blue were obtained from Serva (Heidelberg; Germany); 1-ethyl-3-[3-dimethylaminopropyl] carbodiimide (EDC) (#22980, PIERCE, Rockford, IL; USA), E-64 Sirius Red F3BA (Direct Red 80) and Rhodamine 123 from Sigma–Aldrich (Taufkirchen; Germany); EZ-Link Amine-PEO-Biotin labeling reagent (#21346; PIERCE, Rockford, IL; USA); *Z*-Phe-Arg-AMC from Bachem (King of Prussia, PA, USA).

2.2. Sponges

Spicules (giant basal spicules and comitalia) from the hexactinellids *M. chuni* (Porifera:Hexactinellida:Amphidiscosida:Monorhaphididae) and *M. intermedia* were used as described (Müller et al., 2007a). The *Monorhaphis* sponges reach average sizes of 1.5 m (Fig. 1B). Around the 1.5-m long giant basal spicule (also termed basalia) the cylindrical body of the sponge is attached. The largest spicules within the body of *M. chuni* are the comitalia, parenchymal diactin spicules. The latter spicules are located in the choanosome and reach a maximal size of 60 mm; they have also been termed principalia and comprise the same structure like the giant basal spicules (Müller et al., 2007a). For

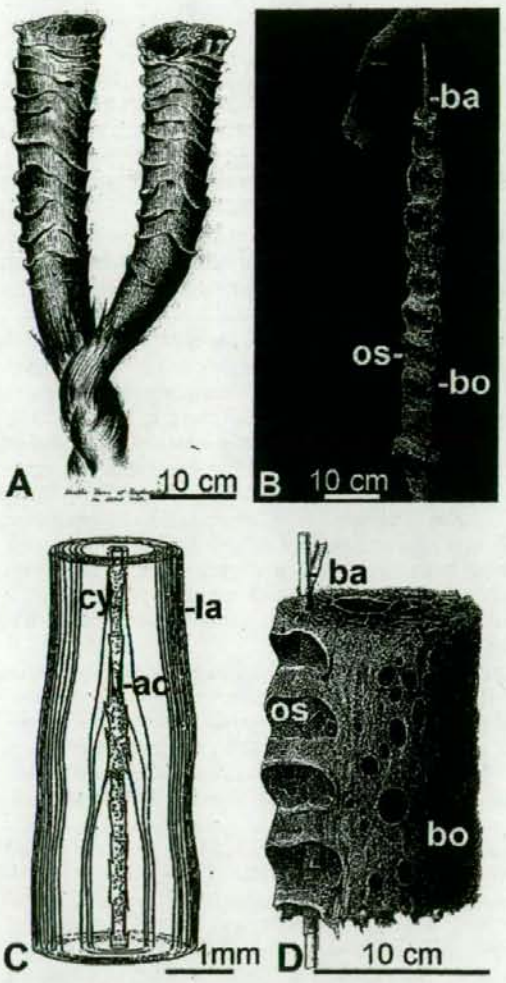

Fig. 1. The two hexactinellid sponge species, used for biophysical, biomechanical and biochemical studies. (A) *Euplectella aspergillum*; the up to 25 cm high specimens live in depths down to 5000 m. Here (one of) the oldest illustrations from Chimmo (1878) is reproduced which shows a non-typical bifurcated specimen found around the Philippine Islands in a depth of 250 m. (B) *Monorhaphis chuni* from the collection of Dr. K. Tabachnick (Institute of Oceanology Moscow, Russia). Around the giant basal spicules (basalia, ba) the cylindrical body (bo) of the sponge is arranged which opens with its osculi (os) to the surrounding water. (C) *M. chuni* had been described thoroughly by Schulze (1904). The specimens had been collected during the "Valdivia" expedition (1898–1899) at East Africa (Somalia basin) in a depth of 1600 m. The morphology of the giant basal spicule (diameter of the spicule: 4 mm) is shown with its three sections; (i) the axial canal (ac), (ii) the axial cylinder (cy) and the lamellar zone (la). The axial canal harbors the organic axial filament. (D) The ellipsoid body of *M. chuni* (bo) is shown which is regularly arranged around the giant basal spicule (ba) and which opens with its osculi (os); they are arranged in one line.

the experiments in the 3-point bending assay, giant basal spicules had been used, which had been freshly collected in the South Chinese Sea (Guangzhou Marine Geological Survey; China). Until the experiments they were stored wet (in seawater).

2.3. Spicules and spicule extracts

The spicules were treated with an ultra-sonicator (S3000; IUL Instruments, Königswinter; Germany) to remove loosely attached organic material and then used for the analysis of the collagen sheet attached to their surfaces. This collagen net could be completely removed from the spicules by overnight treatment with 2% (w/v) sodium dodecyl sulphate solution. For stepwise dissolution of the silica, the *Monorhaphis* spicules were treated with hydrofluoric acid (HF) as described (Shimizu et al., 1998; Müller et al., 2007a; Wang et al., 2007). Spicules were placed on plastic slides and treated with 6 M HF/8 M NH_4F until either the complete silica material had been dissolved, or, until the different organic layers were stepwise exposed. At indicated time points, the HF-mediated dissolution process was terminated by replacing the HF solution with 2 M $CaCl_2$. To visualize the released proteins, Coomassie solution (0.1% (w/v) Coomassie Brilliant blue 250; 40% methanol, 10% acetic acid) was added to the HF solution (Müller et al., 2007a). In a parallel series, the $CaCl_2$ solution was supplemented with Sirius Red F3BA (0.1% (w/v) in saturated picric acid), to stain the collagen-like fibers as described (Junqueira et al., 1979; Walsh et al., 1992; Taskiran et al., 1999). Additionally, the organic material in the silica shell of the spicules was stained with Rhodamine 123 (0.01% (w/v) in dimethyl sulfoxide) as described (Schröder et al., 2006). At different times of incubation (up to 40 min) photos from Coomassie- and Sirius Red-stained samples were taken with an Olympus AHBT3 microscope and/or by Nomarsky differential interference contrast (DIC) imaging. The fluorescence of the Rhodamine stained specimens was visualized using the filter pair 489 nm (excitation)/520 nm (emission).

Matrix protein from the lamellar zone of the freshly collected spicules was obtained by partial dissolution of this zone; the HF-treatment was stopped after 3 h. Then the undissolved silica material was removed and the remaining organic material was collected by centrifugation (5000g; 10 min; 4 °C). Both, the supernatant and the sediment (approximately 50 μg of protein), were dissolved in 50 μl $NaDodSO_4$–PAGE sample buffer and then size-separated by $NaDodSO_4$–PAGE. In a separate series of experiments the sediment was dissolved in 6 M urea, supplemented with 10% (v/v) β-mercaptoethanol for 30 min, while heating (60 °C), and again size-separated ($NaDodSO_4$–PAGE).

Samples of individual (single) lamellae were obtained by mechanical treatment of the spicules which chipped off cherts of lamellae from the axial cylinder.

In another set of experiments spicules from *Monorhaphis* were extracted avoiding HF, as described before for *S. domuncula* (Schröder et al., 2006). In brief, the spicules were ground/pulverized thoroughly in a mortar together with lysis-buffer (1× TBS (Tris-buffered saline); pH 7.5, 1 mM EDTA, 1% Nonidet-P40) and subsequently stirred for 1 h at 4 °C.

2.4. Electron microscopy

Three millimetres (giant basal spicule) or 500 μm (comitalia) thick spicules were embedded in an epoxy resin (Struble and Stutzman, 1989) and sliced (Müller et al., 2007a). The surfaces of the cross sections were polished with emery paper (Siliconcarbide; Matador, Hoppenstedt, Darmstadt, Germany) and the quality of the surface was inspected under a stereomicroscope with an enlargement of about 30×. Backscattered analysis was performed with this microscope using 15-keV beam voltage and 50 μA emission current at a working distance of 6 mm (Holmes et al., 1987).

In one experiment the spicule was broken to allow a tangential view of the fractured surface. Scanning electron microscopy (SEM) analysis of spicules was performed with a Zeiss DSM 962 Digital Scanning Microscope (Zeiss, Aalen; Germany). The samples were mounted onto aluminum stubs (SEM-Stubs G031Z; Plano, Wetzlar; Germany) that had been covered with adhesive carbon (carbon adhesive Leit-Tabs G3347). Then the samples were sputtered with a 10-nm thin layer of gold in argon plasma (Bal Tec Med 020 coating system; Bal Tec, Balzers, Liechtenstein). The high resolution SEM (HRSEM) analysis was carried out using a broken spicule, which had not been polished with emery paper, in a LEO 1530 Gemini field-emission scanning electron microscope (FESEM). An energy within the range 1 and 5 kV of extraction voltage was applied; in this range no change in the images could be recorded. The signals were detected (in-lens annular, secondary electron) and processed (pixel averaging, frame integration/continuous averaging). In order to reach high morphological resolution, small pieces from spicules were fastened with conductive carbon tabs on aluminum sample holders. Samples were prepared by placing a drop of material on silicon wafers. For better conductivity, the samples were sputtered with 8 nm of gold using a Baltec MED020 coating system.

2.5. EDX analysis

Energy dispersive X-ray (EDX) analysis of the collagen layer was performed on SEM images (backscattered mode) using a Philips XL 30 ESEM microscope because this is able to image uncoated and hydrated samples by means of a differential pumping system and a gaseous secondary electron detector. ESEM offers full functionality in the three modes of operation: high vacuum, low vacuum, and ESEM mode. A low-vacuum mode is suitable for the examination of uncoated nonconductive samples. ESEM mode allows very high chamber pressures up to 20 Torr (Rädlein and Frischat, 1997; Tahir et al., 2005; Ni et al., 2006).